AFRL-RH-WP-TR-2019-0038

SILVER NANOPARTICLE SURFACE COATINGS EFFECT ON MITOCHONDRIAL STRUCTURE AND FUNCTION

Mary E. Huddleston, Richard L. Salisbury

Henry M. Jackson Foundation

Melinda E. Meiring

Department of Neuroscience

M. Tyler Nelson, Saber M. Hussain

Human Signatures Branch

May 2019
Interim Report

AIR FORCE RESEARCH LABORATORY
711TH HUMAN PERFORMANCE WING,
AIRMAN SYSTEMS DIRECTORATE,
WRIGHT-PATTERSON AIR FORCE BASE, OH 45433
AIR FORCE MATERIEL COMMAND
UNITED STATES AIR FORCE

NOTICE AND SIGNATURE PAGE

Using Government drawings, specifications, or other data included in this document for any purpose other than Government procurement does not in any way obligate the U.S. Government. The fact that the Government formulated or supplied the drawings, specifications, or other data does not license the holder or any other person or corporation; or convey any rights or permission to manufacture, use, or sell any patented invention that may relate to them.

This report was cleared for public release by the 88th Air Base Wing Public Affairs Office and is available to the general public, including foreign nationals. Copies may be obtained from the Defense Technical Information Center (DTIC) (http://www.dtic.mil).

AFRL-RH-WP-TR-2019-0038 HAS BEEN REVIEWED AND IS APPROVED FOR PUBLICATION IN ACCORDANCE WITH ASSIGNED DISTRIBUTION STATEMENT.

HUSSAIN.SABER.M.1283223406 Digitally signed by HUSSAIN.SABER.M.1283223406 Date: 2019.09.05 11:13:11 -04'00'

SABER HUSSAIN, Work Unit Manager
Human Signatures Branch
Airman Systems Directorate
711th Human Performance Wing
Air Force Research Laboratory

SIMPSON.RICHARD.D.1091443429 Digitally signed by SIMPSON.RICHARD.D.1091443429 Date: 2019.09.19 09:21:29 -04'00'

RICHARD D. SIMPSON, DR-IV, DAF
Human Centered ISR Division
Airman Systems Directorate
711th Human Performance Wing
Air Force Research Laboratory

This report is published in the interest of scientific and technical information exchange, and its publication does not constitute the Government's approval or disapproval of its ideas or findings.

REPORT DOCUMENTATION PAGE

Form Approved
OMB No. 0704-0188

1. REPORT DATE *(DD-MM-YY)*	2. REPORT TYPE	3. DATES COVERED *(From - To)*
01 05 19	Interim Report	August 2016 – February 2019

4. TITLE AND SUBTITLE
Silver nanoparticle surface coatings effect on mitochondrial structure and function

5a. CONTRACT NUMBER
In-House-

5b. GRANT NUMBER

5c. PROGRAM ELEMENT NUMBER
61102F

6. AUTHOR(S)
Mary E. Huddleston[1,2], Melinda E. Meiring[3], M. Tyler Nelson[1], Richard L. Salisbury[1,2], and Saber M. Hussain[1]

5d. PROJECT NUMBER

5e. TASK NUMBER

5f. WORK UNIT NUMBER
H0H3

7. PERFORMING ORGANIZATION NAME(S) AND ADDRESS(ES)
[2] Henry M. Jackson Foundation
for the Advancement of Military Medicine
Wright Patterson Air Force Base, OH

[3] Department of Neuroscience
Cell Biology, and Physiology
Wright State University, Dayton, OH

8. PERFORMING ORGANIZATION REPORT NUMBER

9. SPONSORING/MONITORING AGENCY NAME(S) AND ADDRESS(ES)
[1] Air Force Materiel Command
Air Force Research Laboratory
711th Human Performance Wing
Airman Systems Directorate
Human-Centered ISR Division
Human Signatures Branch
Wright-Patterson AFB, OH 45433

10. SPONSORING/MONITORING AGENCY ACRONYM(S)
711 HPW/RHXB

11. SPONSORING/MONITORING AGENCY REPORT NUMBER(S)
AFRL-RH-WP-TR-2019-0038

12. DISTRIBUTION/AVAILABILITY STATEMENT
Distribution A: Approved for public release. submitted to Toxicological Sciences Journal

13. SUPPLEMENTARY NOTES
Report contains color. 88ABW-2019-2184, cleared on 6 May 2019

14. ABSTRACT
Silver nanoparticles (AgNPs) are widely used in numerous consumer products due to their antimicrobial properties. AgNPs have been shown to be toxic to human cells although this toxicity can be somewhat mitigated by coating the nanoparticle surface to prevent Ag ion leakage. It has been suggested that Ag acts on mitochondria to induce the toxic response, however, a comprehensive examination of mitochondria has yet to be carried out. Mitochondria play many important roles in cells including energy production, regulation of reactive oxygen species, and apoptotic signaling. Mitochondria function is intimately tied to maintenance of mitochondrial structure which includes mitochondrial dynamics and ultrastructure. This study aims to examine mitochondria function and structure after the treatment of A549 cells with Ag coated with citrate, PVP, and BPEI to determine if the different surface coatings elicit different toxicological responses. Ag BPEI was the most toxic of the three coatings as it increased cell death, decreased mitochondrial membrane potential, and impacted mitochondrial ultrastructure. Ag citrate and Ag PVP had similar toxic responses to mitochondrial ultrastructure with Ag citrate being slightly more toxic as it entered cells sooner and caused an increase to mitochondrial area.

15. SUBJECT TERMS
silver nanoparticles, mitochondria, mitochondrial ultrastructure

16. SECURITY CLASSIFICATION OF:			17. LIMITATION OF ABSTRACT:	18. NUMBER OF PAGES	19a. NAME OF RESPONSIBLE PERSON (Monitor)
a. REPORT	b. ABSTRACT	c. THIS PAGE			Saber Hussain
U	U	U	SAR	33	19b. TELEPHONE NUMBER *(Include Area Code)* N/A

Standard Form 298 (Rev. 8-98)
Prescribed by ANSI Std. Z39-18

Contents

1 Introduction

Silver nanoparticles (AgNPs) are used in a large number of products including textiles, cosmetics, bandages, kitchenware, electronics, and medical supplies largely due to their antimicrobial properties (Foldbjerg and Autrup 2013; Quadros and Marr 2010). This quality is largely attributed to AgNPs tendency to leach silver ions which are detrimental to the integrity of the bacterial cell wall (El Badawy et al. 2011; Foldbjerg and Autrup 2013; Quadros and Marr 2010; Silva et al. 2014). Silver ions have been shown in many studies to also be toxic to human and mammalian cells *in vitro* and *in vivo* (Ahamed et al. 2008; Beer et al. 2012; Braydich-Stolle et al. 2014; Comfort et al. 2014; Dong et al. 2016; Foldbjerg and Autrup 2013; Hussain et al. 2005; Kovacs et al. 2016; Park et al. 2010; Yoisungnern et al. 2015). The large number of products containing AgNPs increases the risk of exposure. One of several ways AgNPs can enter the body is through inhalation. To focus on this mode of exposure, A549 human lung adenocarcinoma epithelial cells were used in this study (Holder and Marr 2013; Quadros and Marr 2010) as 50 nm AgNPs have a 40% disposition efficiency in the alveolar region of the lung after inhalation (Quadros and Marr 2010). To combat toxicity, AgNPs are often coated in chemicals to facilitate dispersion and prevent ion leakage (Foldbjerg and Autrup 2013; Kvítek et al. 2008; Tejamaya et al. 2012). Citrate, polyvinylpyrrolidone (PVP), and branched polyethylenimine (BPEI) are some commonly used coatings that have been shown to reduce but not mitigate AgNP toxicity (Anderson et al. 2015; Chairuangkitti et al. 2013; El Badawy et al. 2011; Foldbjerg and Autrup 2013; Huk et al. 2015; Huk et al. 2014; Silva et al. 2014; Suliman et al. 2015; Tejamaya et al. 2012; Wang et al. 2014).

Previous literature has focused on oxidative stress, lipid peroxidation, and cellular metabolism as evidence for AgNP cytotoxicity implicating mitochondria as a likely source of the

Ag toxicological pathway (Dong et al. 2016; Foldbjerg and Autrup 2013; Hsin et al. 2008; Kovacs et al. 2016; Quadros and Marr 2010; Yoisungnern et al. 2015). Treatment with AgNPs has shown to lower mitochondrial membrane potential ($\Delta\Psi_m$), increase cellular reactive oxygen species (ROS), and decrease mitochondrial function (Chairuangkitti et al. 2013; Costa et al. 2010; Dong et al. 2016; Kovacs et al. 2016; Suliman et al. 2015; Teodoro et al. 2011; Yoisungnern et al. 2015). These results have been largely from indirect mitochondrial assays and there have been few direct mitochondrial assessments done (Costa et al. 2010; Teodoro et al. 2011; Yoisungnern et al. 2015). Mitochondria are complex organelles in which form and function are intimately tied. Mitochondria carry out important roles in cells including Ca^{2+} regulation, lipid biosynthesis, ROS maintenance, apoptosis initiation, and cellular metabolism. In order for these processes to be carried out, the mitochondria have to regulate their double membrane structure as well as undergo dynamic fusion and fission to regulate mitochondrial health and to meet the energy demands of the cell. In order to maximize the amount of energy produced, the inner membrane has a much greater surface area than the mitochondrial outer membrane causing the inner membrane to exist in folds known as cristae. Loss of the cristae ultrastructure has been long associated with mitochondrial dysfunction and cellular apoptosis (Brookes et al. 2004; Detmer and Chan 2007; Karbowski and Youle 2003; Sun et al. 2007; Zick et al. 2009). In order to better understand AgNP effects on mitochondria and the role NP coatings play, this study utilized functional as well as structural analysis of these organelles.

2 Materials and Methods

2.1 Cell culture and treatment conditions

A549 alveolar-like type II lung epithelial cells (American Type Culture Collection, VA, USA) were cultured in T75 flasks with RPMI-1670/10% FBS/1% penicillin/streptomycin (p/s) cell culture medium (Gibco, Fisher Scientific, USA) and maintained in an incubator at 37°C under 5% CO_2. Cells were released from flasks using 0.25% Trypsin-EDTA (Invitrogen, USA) for 5 min at 37°C and seeded into welled plates for 24 hours. 50 nm BioPure Ag citrate, 50 nm BioPure Ag BPEI, and 50 nm NanoXact, dried Ag PVP were purchased from NanoComposix. 1 mg/ml aqueous AgNP solutions were vortexed for 1 min and used to make 50 µg/ml and 5 µg/ml solutions in complete cell culture medium. Prior to exposure the nanoparticle solutions were vortexed for 20 sec. Cells were treated with 5 µg/ml and 50 µg/ml 50 nm Ag coated with either citrate, PVP, or BPEI for 4 and 24 hours. Control cells included untreated cells cultured with the vehicle (5% ddH_2O), 50 µg/ml Ag nitrate (Sigma-Aldrich, USA) as an uncoated Ag positive control, 4 µM staurosporine (STS, Selleckchem, USA) for 3 hours as a positive control for apoptosis, 80 µg/ml antimycin A (overnight, Sigma-Aldrich, USA) as a positive control for inhibiting electron transport resulting in mitochondrial fragmentation and loss of $\Delta\Psi_m$, and 80 µM mdivi-1 (overnight, Selleckchem, USA) as a positive control for mitochondrial fusion.

2.2 Nanoparticle characterization

50 nm AgNPs were dropped onto 200 mesh Cu grids and allowed to dry. Size and shape were confirmed with transmission electron microscopy (TEM). Dynamic light scattering (DLS) was used to characterize the hydrodynamic diameter and zeta potential of the nanoparticles in culture media and ddH_2O for 3 independent experiments.

2.3 Quantification of NP toxicity

Flow cytometry was used to measure $\Delta\Psi_m$, apoptosis, and cell death with Guava EasyCyte 12HT flow cytometer using the Millipore FlowCellect MitoDamage kit (Millipore Sigma, USA). Cells were seeded at 1.5 X 10^5 cell/ml in a 24 well plate and stained following the protocol per the Millipore MitoDamage kit instructions with minor changes. Briefly, the media and cells were collected from the welled plate and pelleted in microcentrifuge tubes. The cells were resuspended in 60 µl 1X Assay Buffer and mixed with 60 µl MitoDamage working solution. The cells were washed once and resuspended in 600 µl 1X Assay buffer. 200 µl of the stained cell suspensions were moved to a 96-well U-bottom plate, stained with 3 µl 7-AAD, and placed in the flow cytometer. The kit contains MitoSense Red, Annexin V, and 7-AAD to measure impaired $\Delta\Psi_m$, apoptosis, and cell death respectively. One well of untreated cells were lysed with 1X RIPA lysis buffer (Millipore Sigma, USA) as a gating control. Gates were adjusted using untreated, lysed, and damaged $\Delta\Psi_m$ controls in the InCyte software. 3000 events were collected from 3 independent experiments each with 2 replicates.

2.4 Live cell metabolic analysis

The oxygen consumption rate (OCR) was measured by Seahorse XF96 analyzer in order to quantify mitochondrial function. Cells were seeded at 1 X 10^5 cells/ml in 96 well Seahorse cell culture plates. Cells were prepared according to the protocol laid out in the Agilent Mito Stress Test kit (Agilent, USA) using 1 µM oligomycin, 1 µM carbonyl cyanide-p-trifluoromethoxyphenylhydrazone (FCCP), and 0.9 µM rotenone/antimycin A determined after optimization. The four main properties of mitochondrial respiration that the Seahorse XF96 analyzer measures are basal respiration, ATP turnover, proton leak, and maximal respiration. Basal respiration is the oxygen consumed by ATP synthase, proton leak, and substrate oxidation.

The addition of oligomycin inhibits ATP synthase causing a change in OCR that is proportional to the rate of ATP turnover. FCCP is a proton ionophore which allows the mitochondrial inner membrane to be permeable to protons causing oxygen to be consumed rapidly. This calculates the maximal respiration that can be sustained by the cells. The last injection of rotenone and antimycin A inhibits the electron transport chain and shuts down all oxygen consumption performed by mitochondria. This determines the non-mitochondrial respiration which is subtracted from basal respiration, ATP turnover, proton leak, and maximal respiration. Subtracting non-mitochondrial respiration from the OCR after oligomycin injection calculates the proportion of basal respiration attributed to proton leak. Proton leak is the oxygen consumed by protons crossing the mitochondrial inner membrane without net ATP synthesis. And so, mitochondrial function can by analyzed from these parameters. Normalization was done based on cell count per well by addition of 2 µg/ml (final well concentration) Hoechst 33342 (Invitrogen, USA) and automatic cell counting of an image from the center of the well on the BioTek Cytation 5 using 4X objective and DAPI filter. Total cell number per well was calculated by multiplying cells in image by a factor of 3.71 which is the fold change from area covered by cells in each well (10.67 mm^2) divided by dimension of image (2.876 mm^2). 3 independent experiments each with 4 replicates were performed.

2.5 Semi-quantification of mitochondrial dynamics

Fluorescent microscopy was used to determine if the silver coatings caused a change in the balance of mitochondrial fusion and fission. Cells were seeded at 7.6 X 10^4 cells/ml on glass coverslips in 24-well plates. Cells were stained with 400 nM MitoTracker H_2CMXRos (Invitrogen, USA) for 1 hour at 37°C then fixed with 4% paraformaldehyde (EMS, USA). After permeabilization with 0.2% Triton X-100 (LabChem, USA) and blocking with 1% BSA in PBS

(Sigma-Aldrich, USA), cells were stained with 1:1000 Alexa Fluor Phalloidin 488 (Invitrogen, USA) and 300 nM DAPI (ThermoFisher, USA). Cover slips were mounted to glass slides with ProLong Diamond (Invitrogen, USA) and imaged with PlanApo N 60 X oil objective on Olympus Fluoview 1000 confocal microscope (Dolman et al. 2013; Fine-Coulson et al. 2015). Laser settings were kept consistent across samples. Mitochondrial elongation and interconnectivity were quantified with the ImageJ macro Mitochondria Morphology designed by Dagda et al. (2009). Images were collected from 3 independent experiments each with 2 replicates. At least 40 cells were manually circled for each treatment, the red channel isolated, and threshold set with the MaxEntropy selection on ImageJ. The macro measured average perimeter, circularity, and area of the mitochondria in the cell. Average circularity defines the index of elongation and average area/perimeter ratio defines the index of interconnectivity.

2.6 Nanoparticle uptake and mitochondrial ultrastructure analysis

TEM was used to confirm NP uptake of AgNPs and to quantify changes to mitochondrial ultrastructure. The procedure for processing cells for TEM was modified from several sources (Collet 1979; Gualtieri et al. 2009; Schrand et al. 2010; Sun et al. 2007; Tang et al. 2013; Venable and Coggeshall 1965) to optimize visualization of cristae structures. Cells were seeded at 1.88 X 10^5 cells/ml in 6-well plates and grown overnight. Then cells were exposed to AgNPs, collected, and fixed overnight with 2.5% glutaraldehyde (EMS, USA) in 0.1 M sodium cacodylate buffer (EMS, USA) at 4°C. This was followed by four washes in buffer on ice and post-fix with 1% osmium tetroxide (EMS, USA) in 0.1 M sodium cacodylate buffer supplemented with 3 µM calcium chloride (Acros Organics, USA) and 0.8% potassium ferrocyanide (Acros Organics, USA) for 30 min on ice. Cells were twice washed with buffer followed by two water washes on ice. An *en bloc* stain followed with 1% uranyl acetate (EMS,

USA) for 30 min on ice and another four washes with water at room temperature. The cell pellets were dehydrated with a graded ethanol series and embedded in LR White resin (EMS, USA). Sections were collected on 200 mesh Cu grids and stained with 2% uranyl acetate and 0.4% lead citrate (EMS, USA). Images and energy dispersive X-ray spectroscopy were collected on Fei Talos F200X TEM and mitochondrial quantification was done using ImageJ of 10 cells per treatment which was about 150-200 mitochondria per treatment.

2.7 Statistics

One-way ANOVA with a Dunnett's multiple comparisons test between untreated and treated cells and Tukey's multiple comparisons test within each concentration at 95% confidence interval were calculated using GraphPad Prism.

3 Results

3.1 AgNP characterization and uptake

Nanoparticle toxicity is influenced by many different factors including size, shape, coating, and charge (Foldbjerg and Autrup 2013; Quadros and Marr 2010). It is therefore important to understand these characteristics of a given nanoparticle treatment before being able to discuss its toxicological implications. In order to focus on the impact surface coating has on mitochondrial structure and function, three NPs with the same size and shape were chosen. The 50 nm size was confirmed by TEM (Figure 1) in which the three different AgNPs were observed to all be spherical and composed of silver. The BPEI coating is also visible with TEM. NPs have been shown to agglomerate when in cell culture media due to the interaction of the NPs with proteins in the media and the charge of the NPs themselves (El Badawy et al. 2011; Foldbjerg and Autrup 2013; Quadros and Marr 2010). In water, Ag citrate and Ag BPEI were around 50 nm and 60 nm respectively while Ag PVP was around 96 nm (Table 1). Dispersion in media changed the hydrodynamic size of Ag citrate to 75 nm and Ag BPEI to 150 nm. In water, the zeta potentials of Ag citrate, PVP, and BPEI were -40 mV, -10 mV, and 35 mV respectively. However, these AgNPs zeta potentials were neutralized to similar charges in cell culture media (Table 1).

In the cells examined, Ag BPEI was observed in cells at both concentrations and time points. Ag citrate was also observed in A549 cells but only at 50 µg/ml. No Ag PVP was observed in the cells examined. The majority of AgNPs were located in vesicles in the cytoplasm and none were observed in mitochondria (Figure 2).

3.2 AgNPs effect mitochondrial membrane potential and cell viability

There is evidence that AgNPs effect $\Delta\Psi_m$ and cell viability (Chairuangkitti et al. 2013; Dong et al. 2016; Kovacs et al. 2016; Suliman et al. 2015; Teodoro et al. 2011; Yoisungnern et

al. 2015). Flow cytometry was used to determine if citrate, PVP, or BPEI coatings aggravated or alleviated these effects. Using MitoSense Red, which loses fluorescence as $\Delta\Psi_m$ decreases, we were able to determine that these AgNPs did not lead to an increase in cells with damaged $\Delta\Psi_m$ after 4 hour at either the high or low dose (Figure 3B). After 24 hours, 50 µg/ml Ag BPEI significantly increased the percentage of cells with damaged $\Delta\Psi_m$ compared to control although the effect was small (Figure 3C). The Ag coatings were less toxic than uncoated Ag as treating the cells with Ag nitrate did statistically significant damage to $\Delta\Psi_m$ at 24 hours. Ag BPEI was slightly more toxic to cell health than citrate or PVP coated Ag as 50 µg/ml Ag BPEI had a small but significant increase in the percentage of dead cells compared to the other coatings at both time points and compared to untreated after 24 hour. 5 µg/ml Ag BPEI also displayed a statistically significant increase in cell death compared to 5 µg/ml Ag citrate after 24 hours. The Ag coatings did not cause a statistically significant change to the number of apoptotic cells measured by annexin V staining at either time point or concentration.

3.3 AgNPs do not effect mitochondrial function

Since the AgNPs caused variable changes in $\Delta\Psi_m$, we next examined whether AgNPs alter mitochondrial function. Live cell metabolic analysis quantifies mitochondrial function in a population of cells by measuring oxygen consumption rate. As expected, Ag nitrate caused cells to have almost no mitochondrial function as a large proportion of the cells are dead (Figure 4). 80 µM mdivi-1 caused cells to have a lower basal respiration, ATP turnover, and maximal respiration. However, there were no significant differences in mitochondrial function between the untreated and AgNP treated cells.

3.4 AgNPs cause changes to mitochondrial dynamics

Fluorescent microscopy was used to measure changes in mitochondrial fusion and fission to ascertain whether these toxicological effects corresponded to structural changes. Ag nitrate and antimycin A both significantly decreased interconnectivity at both time points and mdivi-1 and STS significantly decreased interconnectivity after 4 hours (Figure 5). These results are in line with findings previously published (Cassidy-Stone et al. 2008; De Vos et al. 2005; Rehman et al. 2012). AgNPs coated with citrate, PVP, and BPEI did not significantly affect elongation or interconnectivity at either concentration or time point. However, there may be a biological significance after 4 hour as Ag BPEI appears to display more interconnectivity compared to Ag citrate and PVP at both 5 µg/ml and 50 µg/ml.

3.5 AgNPs are taken up by lung cells and effect mitochondrial ultrastructure

A549 cells were examined using TEM to determine if AgNPs cause changes to mitochondrial ultrastructure. Five cristae altered morphological states were identified and categorized for quantification. Normal mitochondria consist of an outer membrane in close conjunction with the inner membrane. This forms two distinct compartments within the mitochondrion with the intermembrane space between the outer and inner membrane and mitochondrial matrix within the inner membrane. The inner membrane folds forming cristae within the matrix which also forms an intra cristae space that is continuous with the inter membrane space. Normal mitochondria are defined as having lamellar cristae with little intra-cristae space (Figure 6A). Normal-vesicular mitochondria have cristae that have started to swell (Figure 6B). Vesicular mitochondria have vesicle-like cristae (Figure 6C). Vesicular-swollen mitochondria have vesicle-like cristae with a portion of the mitochondrion haven lost cristae structure (Figure 6D). Swollen mitochondria have lost almost or all cristae structure (Figure 6E).

Normal-swollen mitochondria have lamellar cristae but unlike normal mitochondria, these also have a portion of the organelle that has swollen (Figure 6F). Cells treated with 50 µg/ml Ag nitrate had lost almost all cellular structure and do not contain any structures that can be defined as mitochondria (Figure 6G).

After 4 hours of treatment with AgNPs, all coatings and concentrations had a significantly decreased number of normal mitochondria compared to untreated cells (Figure 7A). 5 µg/ml Ag BPEI and 50 µg/ml Ag PVP had significantly more normal-vesicular mitochondria than untreated cells. All NPs (with the exception of 50 µg/ml Ag PVP) had significantly more vesicular mitochondria than untreated cells and 5 µg/ml Ag BPEI treated cells had significantly more than Ag citrate or PVP at the same concentration. 5 µg/ml Ag citrate, 5 µg/ml Ag PVP, 50 µg/ml Ag PVP, and 50 µg/ml Ag BPEI had significantly more swollen mitochondria than untreated cells. 5 µg/ml Ag BPEI had significantly less swollen mitochondria than the other AgNPs at the same concentration and time point.

After cells have been treated for 24 hours, the NP treated cells did not have significantly different percentages of normal mitochondria than untreated cells (Figure 7B). However, 50 µg/ml Ag PVP had significantly more normal-vesicular mitochondria compared to untreated cells or other AgNPs at that concentration and 50 µg/ml Ag BPEI had significantly more swollen mitochondria compared to untreated cells or 50 µg/ml Ag PVP.

In addition to changes to cristae structure, mitochondrial area was also quantified from the TEM images. After 4 hour, 5 µg/ml Ag BPEI and 50 µg/ml Ag citrate caused mitochondria to have a significantly greater area compared to untreated cells or to the other Ag coatings within the same concentration (Figure 8A). After 24 hour, 5 µg/ml citrate and PVP, 50 µg/ml citrate and

BPEI had significantly greater mitochondrial area than untreated cells (Figure 8B). 50 µg/ml Ag BPEI was also significantly greater than 50 µg/ml Ag PVP.

4 Discussion

The heterogeneity of nanoparticle physiochemical characteristics and testing methodology makes NP toxicity assessment and cross-referencing challenging. Based on previous literature, we hypothesized that Ag BPEI would be the most toxic due to its positive charge as compared to Ag citrate (negatively charged) or Ag PVP (neutral) (Anderson et al. 2015; El Badawy et al. 2011; Huk et al. 2015; Silva et al. 2014; Wang et al. 2014). AgNPs size was held constant across the different chemical compositions tested to eliminate size as an experimental variable of toxicity. As expected, Ag citrate, PVP, and BPEI had slightly different hydrodynamic sizes in cell culture media, likely due to protein fouling dependent on surface charge, yet all had a similar zeta potential (El Badawy et al. 2011). As such, any effects observed can be attributed to the type of coating on the silver.

Initial observations suggest there are differences between these three coatings. Ag BPEI enters A549 cells more easily as it was observed in cells at the lower concentration. Ag citrate was seen in cells at the higher concentration at both time points but Ag PVP was not observed in any of the 10 cells imaged. Ag PVP might be ionized outside the cell in these conditions but these general observations would need to be quantified and confirmed with other methods such as ICP-MS. The difference in uptake does suggest a variable toxicological response to these differently coated AgNPs.

BPEI caused a change in $\Delta\Psi_m$ after 24 hours at the higher concentration of 50 µg/ml while Ag citrate and Ag PVP did not affect viability or $\Delta\Psi_m$. This supports our hypothesis and is in line with previous studies as Ag BPEI decreased bacteria viability more than Ag citrate and Ag PVP (El Badawy et al. 2011; Silva et al. 2014). Other studies have found Ag citrate and Ag PVP to effect $\Delta\Psi_m$ and cell viability, however the differences in NP size and testing conditions

can greatly influence NP toxicity. For example, a mixture of 40-90 nm Ag PVP did not significantly decrease $\Delta\Psi_m$ at concentrations lower than 50 µg/ml after 24 hours (Chairuangkitti et al. 2013) and only significantly decreased viability to 80% in A549 cells (Chairuangkitti et al. 2013; Suliman et al. 2015). 10 nm Ag citrate significantly decreased relative growth of TK6 cells after 24 hours at concentrations greater than 4 µg/ml (Huk et al. 2015), but that is not surprising considering smaller NPs are more toxic (Huk et al. 2014; Kovacs et al. 2016). While 50 nm Ag BPEI causes significantly more cell death at 24 hours compared to untreated cells, it is less than Ag nitrate, which supports coated Ag being less toxic (Braydich-Stolle et al. 2014; Comfort et al. 2014). Interestingly, 50 nm AgNPs coated with citrate, PVP, or BPEI did not induce apoptosis at these time points or concentrations in these cells. Other studies found that 50 µg/ml 40-80 nm Ag PVP significantly increased caspase-3 and caspase-9 activity (markers of apoptosis) in A549 cells after 24 hours (Suliman et al. 2015) and 5 and 35 nm Ag citrate significantly increased caspase-3 cleavage and annexin V staining in osteosarcoma cells after 24 hours (Kovacs et al. 2016). The AgNPs from these previous studies are probably more toxic due to the smaller size resulting in more apoptotic activity, loss of $\Delta\Psi_m$, and cell viability.

The change to $\Delta\Psi_m$ would suggest Ag BPEI would cause a change to mitochondrial function as well. However, live cell metabolic analysis measurements detected no significant differences between untreated cells and those exposed to coated AgNPs. This would seem to be in opposition to previous results in which 40 nm and 80 nm AgNPs caused a significant decrease in basal respiration at 2 and 5 ug/mg protein in isolated rat liver mitochondria (Teodoro et al. 2011). However, the results of the previous and current study cannot really be compared since the conditions to keep isolated mitochondria stable are different than the cellular environment and this confers different properties to NPs effecting the toxicity. Live cell metabolic analysis

using Seahorse XF is a relatively new technology and has only recently been used with nanoparticles (Chi et al. 2013; Lindeque et al. 2018; Lu et al. 2015; Tucci et al. 2013; Wang et al. 2015; Zhou et al. 2014). The assay has been greatly optimized in the last 10 years, so some of the earlier papers did not set the assay up properly or normalize the data to either protein concentration, mitochondrial content, or cell number (Chi et al. 2013; Lu et al. 2015; Tucci et al. 2013; Wang et al. 2015). However, significant differences in mitochondrial function were observed between untreated cells and human breast cancer cells treated with gold nanorods (Zhou et al. 2014), irradiated A549 cells treated with iron oxide nanoparticles (Hauser et al. 2016), and HepG2 cells treated with citrate or PVP coated gold nanoparticles (Lindeque et al. 2018). The fact that the current study did not detect any functional changes is probably due to Ag BPEI only causing a small significant increase in the number of cells with damaged $\Delta\Psi_m$. The flow cytometer reads $\Delta\Psi_m$ on a cell by cell basis so the small percentage of cells with damaged mitochondrial function could be diluted in the OCR measurement from a population of cells. Live cell metabolic analysis does have its advantages as it can measure changes to respiration in whole cells, however it is probably better utilized with more toxic treatments.

The difference in $\Delta\Psi_m$ suggests that mitochondrial structure could be effected in these cells even though mitochondrial function was not affected by these AgNPs. One aspect of mitochondrial structure involves the dynamic nature of the mitochondrial network within the cell. Mitochondrial dynamics are dependent on the organelles' ability to undergo fusion and fission and are important to normal cell function. Fusion is required for the maintenance of mtDNA and can protect cells from stress such as starvation (Rambold et al. 2011) by allowing cells to maximize ATP production. Fission is necessary during cell division to sequester mitochondria into the new cell and is a prerequisite for mitophagy and the mitochondrial directed

apoptosis. An imbalance in mitochondrial dynamics leads to excessive fragmentation or tubulation of the mitochondrial network (Brookes et al. 2004; Detmer and Chan 2007; Karbowski and Youle 2003; Zick et al. 2009). The data suggests that these AgNPs do not effect mitochondrial dynamics as Ag citrate, PVP, and BPEI do not cause a significant change to elongation or interconnectivity. However there is another possible explanation. Meyer et al. (2017) looked at mitochondrial fusion and fission responses to toxicological insults and proposed that a mild toxic response would cause both fusion and fission to increase which would manifest in some assays as no change to mitochondrial dynamics. Ag citrate, PVP, and BPEI could be causing a mild toxic response since there was no significant increase to either fusion or fission detected with the current assay but the AgNPs had an effect on $\Delta\Psi_m$ and viability.

If the AgNPs are initiating a mild toxic response, then it would follow that the AgNPs could cause mitochondrial ultrastructural changes. Sun et al. (2007) measured similar cristae structures after the induction of apoptosis with etoposide in HeLa cells. The authors also tracked cytochrome c release and $\Delta\Psi_m$ in cells with the observed cristae types. Normal mitochondria contained cytochrome c and maintained $\Delta\Psi_m$. As apoptosis progressed, cytochrome c was released, $\Delta\Psi_m$ was maintained, and more mitochondria contained vesicular cristae (Sun et al. 2007). Our data showed that AgNPs caused a significant increase in vesicular cristae without changing $\Delta\Psi_m$. Sun et al. (2007) also showed the percentage of mitochondria with swollen cristae increased once the mitochondria lost $\Delta\Psi_m$. From this we can conclude that these AgNPs cause a toxic effect on mitochondria as all coatings significantly increased the number of mitochondria with swollen and vesicular cristae after 4 hours. Even though Ag BPEI did not significantly increase swollen mitochondria compared to the other coatings at 4 hours, it is still categorized as the most toxic as it does significantly increase swollen mitochondria at 50 µg/ml

after 24 hours which coincides with the damage to $\Delta\Psi_m$. Ag citrate and Ag PVP similarly effected ultrastructure at 4 hours but by 24 hours, 50 µg/ml Ag PVP caused a significant increase to the number of normal-vesicular mitochondria compared to the other coatings suggesting there are slight differences between the positive and neutral coatings. While all three AgNPs caused a decrease in normal mitochondria at 4 hours at both low and high concentrations, this was no longer observed at 24 hours. The increase in both fusion and fission probably altered the cristae structure in cells treated with AgNPs (Detmer and Chan 2007; Zick et al. 2009) but since this was a mild toxic response, the 4 hour mitochondrial defects were corrected by 24 hours. 5 µg/ml Ag BPEI and 50 µg/ml Ag citrate also increased mitochondrial area after 4 hours which is often associated with mitochondrial stress (Chami et al. 2008; Schneeberger et al. 2013; Xu et al. 2011) further supporting the two coatings are more toxic than Ag PVP. These ultrastructural changes were not caused by apoptosis as no significant changes were observed by annexin V staining even though similar structures have been reported after the activation of apoptosis (Sun et al. 2007).

To conclude, Ag citrate, PVP, and BPEI are less toxic then uncoated Ag. We were unable to reject our hypothesis stating Ag BPEI is the most toxic of the three coatings followed by Ag citrate then Ag PVP. Ag BPEI increased cell death, decreased $\Delta\Psi_m$, and caused an increase in the number of swollen mitochondria. Ag citrate and Ag PVP have similar toxic profiles but since Ag citrate effected mitochondrial area at 4 hours it is the more toxic of the two coatings. We also speculate that Ag citrate and Ag PVP might have different mechanisms for the induction of NP toxicity. Based on mitochondrial functional and structural analysis, these AgNPs do not induce apoptosis, but do cause structural changes due to their mild toxicity in A549 cells at 5 µg/ml and 50 µg/ml after 4 hours and 24 hours.

5 References

Ahamed M, Karns M, Goodson M, Rowe J, Hussain SM, Schlager JJ, Hong Y. 2008. DNA damage response to different surface chemistry of silver nanoparticles in mammalian cells. Toxicol Appl Pharmacol. 233(3):404-410.

Anderson DS, Silva RM, Lee D, Edwards PC, Sharmah A, Guo T, Pinkerton KE, Van Winkle LS. 2015. Persistence of silver nanoparticles in the rat lung: Influence of dose, size, and chemical composition. Nanotoxicology. 9(5):591-602.

Beer C, Foldbjerg R, Hayashi Y, Sutherland DS, Autrup H. 2012. Toxicity of silver nanoparticles - nanoparticle or silver ion? Toxicol Lett. 208(3):286-292.

Braydich-Stolle LK, Breitner EK, Comfort KK, Schlager JJ, Hussain SM. 2014. Dynamic characteristics of silver nanoparticles in physiological fluids: Toxicological implications. Langmuir. 30(50):15309-15316.

Brookes PS, Yoon Y, Robotham JL, Anders MW, Sheu SS. 2004. Calcium, atp, and ros: A mitochondrial love-hate triangle. Am J Physiol Cell Physiol. 287(4):C817-833.

Cassidy-Stone A, Chipuk JE, Ingerman E, Song C, Yoo C, Kuwana T, Kurth MJ, Shaw JT, Hinshaw JE, Green DR et al. 2008. Chemical inhibition of the mitochondrial division dynamin reveals its role in bax/bak-dependent mitochondrial outer membrane permeabilization. Dev Cell. 14(2):193-204.

Chairuangkitti P, Lawanprasert S, Roytrakul S, Aueviriyavit S, Phummiratch D, Kulthong K, Chanvorachote P, Maniratanachote R. 2013. Silver nanoparticles induce toxicity in a549 cells via ros-dependent and ros-independent pathways. Toxicol In Vitro. 27(1):330-338.

Chami M, Oules B, Szabadkai G, Tacine R, Rizzuto R, Paterlini-Brechot P. 2008. Role of serca1 truncated isoform in the proapoptotic calcium transfer from er to mitochondria during er stress. Mol Cell. 32(5):641-651.

Chi T-Y, Yeh H-Y, Lin J-J, Jeng US, Hsu S-h. 2013. Amphiphilic silver-delaminated clay nanohybrids and their composites with polyurethane: Physico-chemical and biological evaluations. Journal of Materials Chemistry B. 1(16):2178-2189.

Collet AJ. 1979. Preservation of alveolar type ii pneumocyte lamellar bodies for electron microscopic studies. J Histochem Cytochem. 27(5):989-996.

Comfort KK, Braydich-Stolle LK, Maurer EI, Hussain SM. 2014. Less is more: Long-term in vitro exposure to low levels of silver nanoparticles provides new insights for nanomaterial evaluation. ACS Nano. 8(4):3260-3271.

Costa CS, Ronconi JV, Daufenbach JF, Goncalves CL, Rezin GT, Streck EL, Paula MM. 2010. In vitro effects of silver nanoparticles on the mitochondrial respiratory chain. Mol Cell Biochem. 342(1-2):51-56.

Dagda RK, Cherra SJ, 3rd, Kulich SM, Tandon A, Park D, Chu CT. 2009. Loss of pink1 function promotes mitophagy through effects on oxidative stress and mitochondrial fission. J Biol Chem. 284(20):13843-13855.

De Vos KJ, Allan VJ, Grierson AJ, Sheetz MP. 2005. Mitochondrial function and actin regulate dynamin-related protein 1-dependent mitochondrial fission. Curr Biol. 15(7):678-683.

Detmer SA, Chan DC. 2007. Functions and dysfunctions of mitochondrial dynamics. Nat Rev Mol Cell Biol. 8(11):870-879.

Dolman NJ, Chambers KM, Mandavilli B, Batchelor RH, Janes MS. 2013. Tools and techniques to measure mitophagy using fluorescence microscopy. Autophagy. 9(11):1653-1662.

Dong P, Li JH, Xu SP, Wu XJ, Xiang X, Yang QQ, Jin JC, Liu Y, Jiang FL. 2016. Mitochondrial dysfunction induced by ultra-small silver nanoclusters with a distinct toxic mechanism. J Hazard Mater. 308:139-148.
El Badawy AM, Silva RG, Morris B, Scheckel KG, Suidan MT, Tolaymat TM. 2011. Surface charge-dependent toxicity of silver nanoparticles. Environ Sci Technol. 45(1):283-287.
Fine-Coulson K, Giguere S, Quinn FD, Reaves BJ. 2015. Infection of a549 human type ii epithelial cells with mycobacterium tuberculosis induces changes in mitochondrial morphology, distribution and mass that are dependent on the early secreted antigen, esat-6. Microbes Infect. 17(10):689-697.
Foldbjerg R, Autrup H. 2013. Mechanisms of silver nanoparticle toxicity. Arch Basic Appl Med. 1(1):5-15.
Gualtieri M, Mantecca P, Corvaja V, Longhin E, Perrone MG, Bolzacchini E, Camatini M. 2009. Winter fine particulate matter from milan induces morphological and functional alterations in human pulmonary epithelial cells (a549). Toxicol Lett. 188(1):52-62.
Hauser AK, Mitov MI, Daley EF, McGarry RC, Anderson KW, Hilt JZ. 2016. Targeted iron oxide nanoparticles for the enhancement of radiation therapy. Biomaterials. 105:127-135.
Holder AL, Marr LC. 2013. Toxicity of silver nanoparticles at the air-liquid interface. Biomed Res Int. 2013:328934.
Hsin YH, Chen CF, Huang S, Shih TS, Lai PS, Chueh PJ. 2008. The apoptotic effect of nanosilver is mediated by a ros- and jnk-dependent mechanism involving the mitochondrial pathway in nih3t3 cells. Toxicol Lett. 179(3):130-139.
Huk A, Izak-Nau E, el Yamani N, Uggerud H, Vadset M, Zasonska B, Duschl A, Dusinska M. 2015. Impact of nanosilver on various DNA lesions and hprt gene mutations – effects of charge and surface coating. Particle and Fibre Toxicology. 12(1):25.
Huk A, Izak-Nau E, Reidy B, Boyles M, Duschl A, Lynch I, Dusinska M. 2014. Is the toxic potential of nanosilver dependent on its size? Part Fibre Toxicol. 11:65.
Hussain SM, Hess KL, Gearhart JM, Geiss KT, Schlager JJ. 2005. In vitro toxicity of nanoparticles in brl 3a rat liver cells. Toxicol In Vitro. 19(7):975-983.
Karbowski M, Youle RJ. 2003. Dynamics of mitochondrial morphology in healthy cells and during apoptosis. Cell Death Differ. 10(8):870-880.
Kovacs D, Igaz N, Keskeny C, Belteky P, Toth T, Gaspar R, Madarasz D, Razga Z, Konya Z, Boros IM et al. 2016. Silver nanoparticles defeat p53-positive and p53-negative osteosarcoma cells by triggering mitochondrial stress and apoptosis. Sci Rep. 6:27902.
Kvítek L, Panáček A, Soukupová J, Kolář M, Večeřová R, Prucek R, Holecová M, Zbořil R. 2008. Effect of surfactants and polymers on stability and antibacterial activity of silver nanoparticles (nps). The Journal of Physical Chemistry C. 112(15):5825-5834.
Lindeque JZ, Matthyser A, Mason S, Louw R, Taute CJF. 2018. Metabolomics reveals the depletion of intracellular metabolites in hepg2 cells after treatment with gold nanoparticles. Nanotoxicology. 12(3):251-262.
Lu HY, Chang YJ, Fan NC, Wang LS, Lai NC, Yang CM, Wu LC, Ho JA. 2015. Synergism through combination of chemotherapy and oxidative stress-induced autophagy in a549 lung cancer cells using redox-responsive nanohybrids: A new strategy for cancer therapy. Biomaterials. 42:30-41.
Meyer JN, Leuthner TC, Luz AL. 2017. Mitochondrial fusion, fission, and mitochondrial toxicity. Toxicology. 391:42-53.

Park EJ, Yi J, Kim Y, Choi K, Park K. 2010. Silver nanoparticles induce cytotoxicity by a trojan-horse type mechanism. Toxicol In Vitro. 24(3):872-878.
Quadros ME, Marr LC. 2010. Environmental and human health risks of aerosolized silver nanoparticles. J Air Waste Manag Assoc. 60(7):770-781.
Rambold AS, Kostelecky B, Elia N, Lippincott-Schwartz J. 2011. Tubular network formation protects mitochondria from autophagosomal degradation during nutrient starvation. Proc Natl Acad Sci U S A. 108(25):10190-10195.
Rehman J, Zhang HJ, Toth PT, Zhang Y, Marsboom G, Hong Z, Salgia R, Husain AN, Wietholt C, Archer SL. 2012. Inhibition of mitochondrial fission prevents cell cycle progression in lung cancer. FASEB J. 26(5):2175-2186.
Schneeberger M, Dietrich MO, Sebastian D, Imbernon M, Castano C, Garcia A, Esteban Y, Gonzalez-Franquesa A, Rodriguez IC, Bortolozzi A et al. 2013. Mitofusin 2 in pomc neurons connects er stress with leptin resistance and energy imbalance. Cell. 155(1):172-187.
Schrand AM, Schlager JJ, Dai L, Hussain SM. 2010. Preparation of cells for assessing ultrastructural localization of nanoparticles with transmission electron microscopy. Nat Protoc. 5(4):744-757.
Silva T, Pokhrel LR, Dubey B, Tolaymat TM, Maier KJ, Liu X. 2014. Particle size, surface charge and concentration dependent ecotoxicity of three organo-coated silver nanoparticles: Comparison between general linear model-predicted and observed toxicity. Sci Total Environ. 468-469:968-976.
Suliman YA, Ali D, Alarifi S, Harrath AH, Mansour L, Alwasel SH. 2015. Evaluation of cytotoxic, oxidative stress, proinflammatory and genotoxic effect of silver nanoparticles in human lung epithelial cells. Environ Toxicol. 30(2):149-160.
Sun MG, Williams J, Munoz-Pinedo C, Perkins GA, Brown JM, Ellisman MH, Green DR, Frey TG. 2007. Correlated three-dimensional light and electron microscopy reveals transformation of mitochondria during apoptosis. Nat Cell Biol. 9(9):1057-1065.
Tang Y, Wang F, Jin C, Liang H, Zhong X, Yang Y. 2013. Mitochondrial injury induced by nanosized titanium dioxide in a549 cells and rats. Environ Toxicol Pharmacol. 36(1):66-72.
Tejamaya M, Romer I, Merrifield RC, Lead JR. 2012. Stability of citrate, pvp, and peg coated silver nanoparticles in ecotoxicology media. Environ Sci Technol. 46(13):7011-7017.
Teodoro JS, Simões AM, Duarte FV, Rolo AP, Murdoch RC, Hussain SM, Palmeira CM. 2011. Assessment of the toxicity of silver nanoparticles in vitro: A mitochondrial perspective. Toxicology in Vitro. 25(3):664-670.
Tucci P, Porta G, Agostini M, Dinsdale D, Iavicoli I, Cain K, Finazzi-Agro A, Melino G, Willis A. 2013. Metabolic effects of tio2 nanoparticles, a common component of sunscreens and cosmetics, on human keratinocytes. Cell Death Dis. 4:e549.
Venable JH, Coggeshall R. 1965. A simplified lead citrate stain for use in electron microscopy. J Cell Biol. 25:407-408.
Wang DF, Rong WT, Lu Y, Hou J, Qi SS, Xiao Q, Zhang J, You J, Yu SQ, Xu Q. 2015. Tpgs2k/plga nanoparticles for overcoming multidrug resistance by interfering mitochondria of human alveolar adenocarcinoma cells. ACS Appl Mater Interfaces. 7(7):3888-3901.

Wang X, Ji Z, Chang CH, Zhang H, Wang M, Liao YP, Lin S, Meng H, Li R, Sun B et al. 2014. Use of coated silver nanoparticles to understand the relationship of particle dissolution and bioavailability to cell and lung toxicological potential. Small. 10(2):385-398.

Xu Z, Xu X, Zhong M, Hotchkiss IP, Lewandowski RP, Wagner JG, Bramble LA, Yang Y, Wang A, Harkema JR et al. 2011. Ambient particulate air pollution induces oxidative stress and alterations of mitochondria and gene expression in brown and white adipose tissues. Part Fibre Toxicol. 8:20.

Yoisungnern T, Choi YJ, Han JW, Kang MH, Das J, Gurunathan S, Kwon DN, Cho SG, Park C, Chang WK et al. 2015. Internalization of silver nanoparticles into mouse spermatozoa results in poor fertilization and compromised embryo development. Sci Rep. 5:11170.

Zhou T, Yu M, Zhang B, Wang L, Wu X, Zhou H, Du Y, Hao J, Tu Y, Chen C et al. 2014. Inhibition of cancer cell migration by gold nanorods: Molecular mechanisms and implications for cancer therapy. Advanced Functional Materials. 24(44):6922-6932.

Zick M, Rabl R, Reichert AS. 2009. Cristae formation-linking ultrastructure and function of mitochondria. Biochim Biophys Acta. 1793(1):5-19.

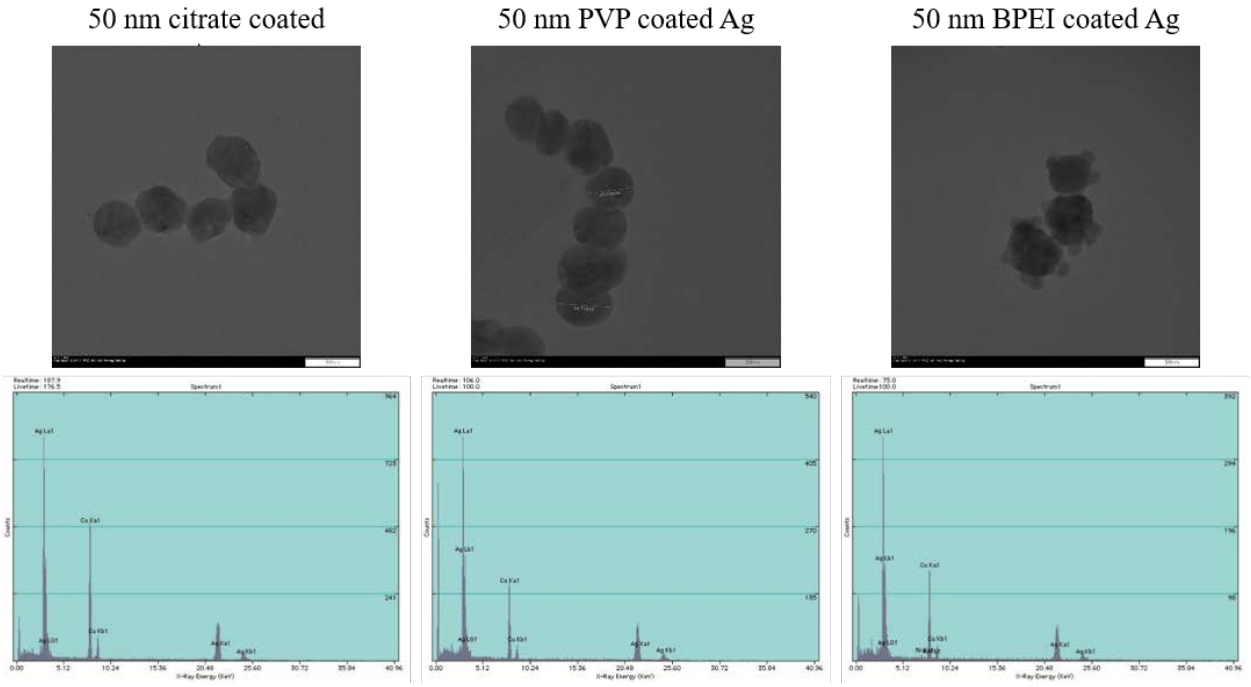

Figure 1. Nanoparticles were confirmed to be 50 nm spherical silver. Representative TEM images of citrate coated silver, PVP coated silver, and BPEI coated silver NPs. Below each TEM image is the corresponding energy dispersive x-ray spectroscopy confirming the NPs are Ag. Scale bar = 50 nm

dispersion in water	hydrodynamic size (d.nm)	zeta potential (mV)
Ag citrate	55.22 ± 2.00	-40.12 ± 0.97
Ag PVP	96.40 ± 1.47	-10.69 ± 1.75
Ag BPEI	64.24 ± 1.67	35.22 ± 6.21
dispersion in media	hydrodynamic size (d.nm)	zeta potential (mV)
Ag citrate	75.36 ± 1.10	-10.37 ± 0.45
Ag PVP	94.57 ± 12.84	-7.50 ± 0.23
Ag BPEI	151.18 ± 23.29	-6.03 ± 3.40

Table 1. Hydrodynamic sizes and zeta potential of silver nanoparticles dispersed in water and in cell culture media. Data displayed are mean of n=3 independent experiments ± SEM

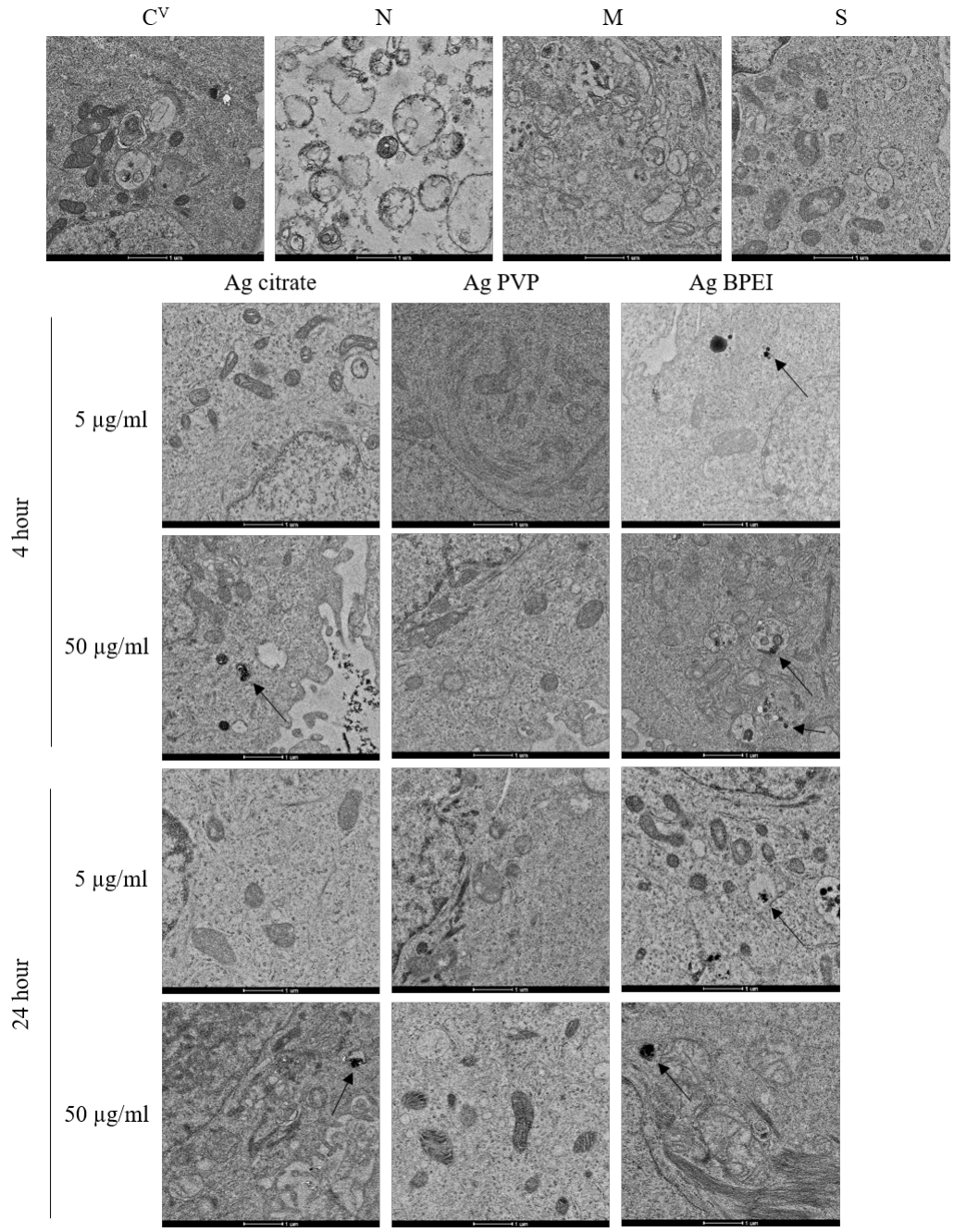

Figure 2. Representative TEM images of cells containing AgNPs. 11,000 X magnification with scale bar = 1 µm. Black arrow points to confirmed AgNPs. C^V=control+vehicle, N=50 µg/ml Ag nitrate, M=80 µM mdivi-1, and S=4 µM staurosporine

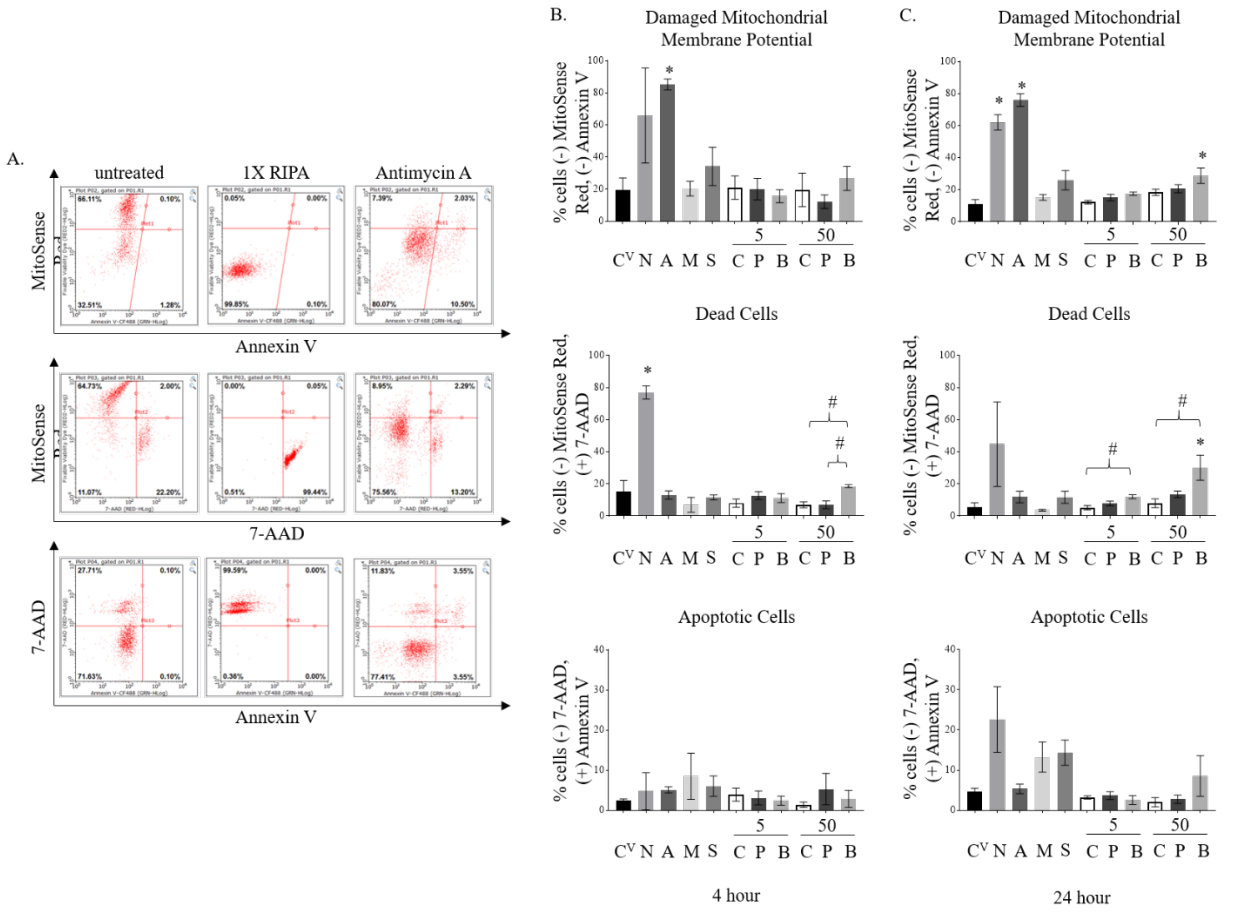

Figure 3. Effects of AgNP coatings on mitochondrial membrane potential and viability. A) Representative images of negative and positive control gating procedure. Untreated cells used as negative control, 1X RIPA buffer for dead positive control, and antimycin A for damaged mitochondrial membrane potential positive control. B) Percentage of total cells with damaged $\Delta\Psi_m$, dead, and apoptotic after 4 hours of exposure with 5 µg/ml and 50 µg/ml AgNPs and C) 24 hours exposure with 5 µg/ml and 50 µg/ml AgNPs. Bar graphs display mean of n=3 independent experiments with SEM. One way ANOVA with multiple comparison tests with * $p<0.05$ compared to control+vehicle using Dunnetts and # $p<0.05$ compared within concentration using Tukey. C^V=control+vehicle, N=50 µg/ml Ag nitrate, A=80 µg/ml antimycin A, M=80 µM mdivi-1, S=4 µM staurosporine, C=Ag citrate, P=Ag PVP, B=Ag BPEI

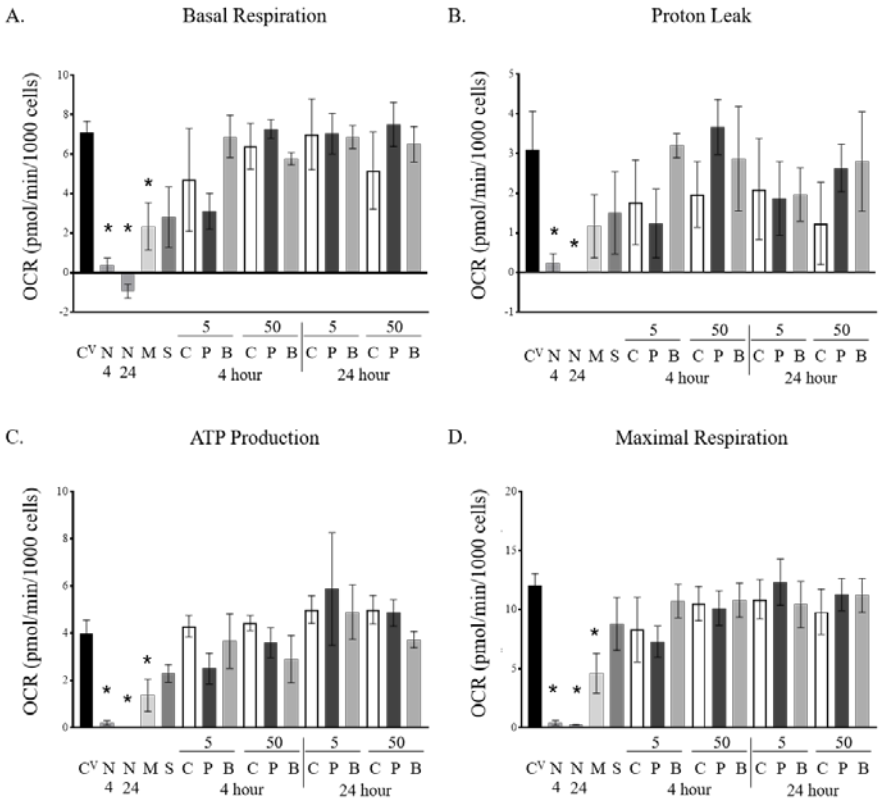

Figure 4. AgNPs impact on mitochondrial respiration. A) Basal oxygen consumption rate (OCR) levels. B) OCR caused by proton leak. C) OCR contributed to ATP production. D) The maximal respiration the mitochondria can achieve. Each well normalized by cell count and displayed as OCR/pmol/min/1,000 cells. Data displayed is an average of n=3 independent experiments each with 4 replicates. One way ANOVA with multiple comparison tests with * $p<0.05$ compared to control+vehicle using Dunnetts and # $p<0.05$ compared within concentration using Tukey. C^V=control+vehicle, N=50 µg/ml Ag nitrate, M=80 µM mdivi-1, S=4 µM staurosporine, C=Ag citrate, P=Ag PVP, B=Ag BPEI

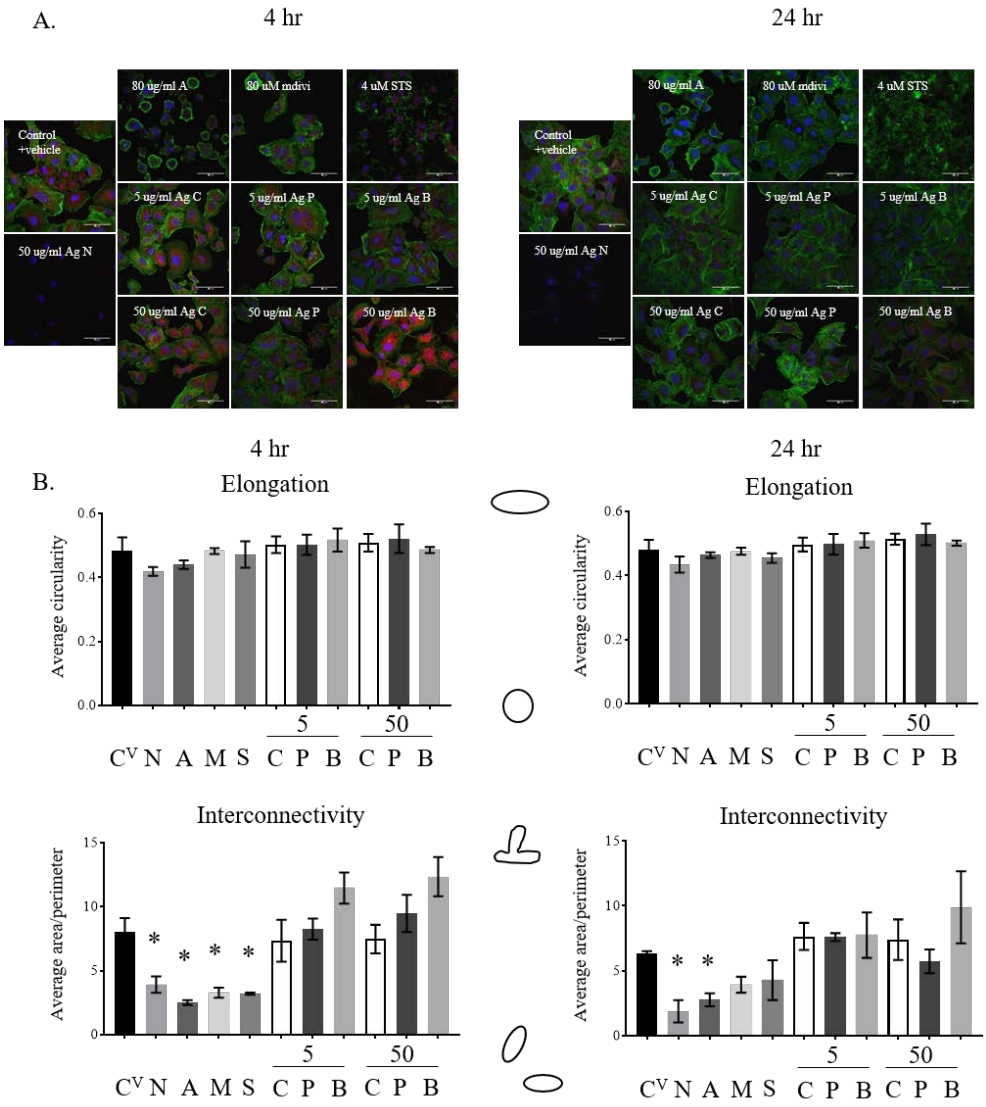

Figure 5. AgNPs do not cause changes to mitochondrial elongation and interconnectivity. Representative fluorescent images of A) 4 hour and 24 hour treatments at 60X magnification. Scale bar = 50 µm. B) Mitochondria elongation measured by the average circularity of mitochondria per cell and mitochondria interconnectivity measured by average area/average perimeter of mitochondria per cell for 4 hours and 24 hours. Mitochondria from at least 40 cells per treatment were measured. Bar graphs display mean of n=3 independent experiments with SEM. One way ANOVA with multiple comparison tests with * $p<0.05$ compared to control+vehicle using Dunnetts and # $p<0.05$ compared within concentration using Tukey. C^V=control+vehicle, N=50 µg/ml Ag nitrate, A=80 µg/ml antimycin A, M=80 µM mdivi-1, S=4 µM staurosporine, C=Ag citrate, P=Ag PVP, B=Ag BPEI

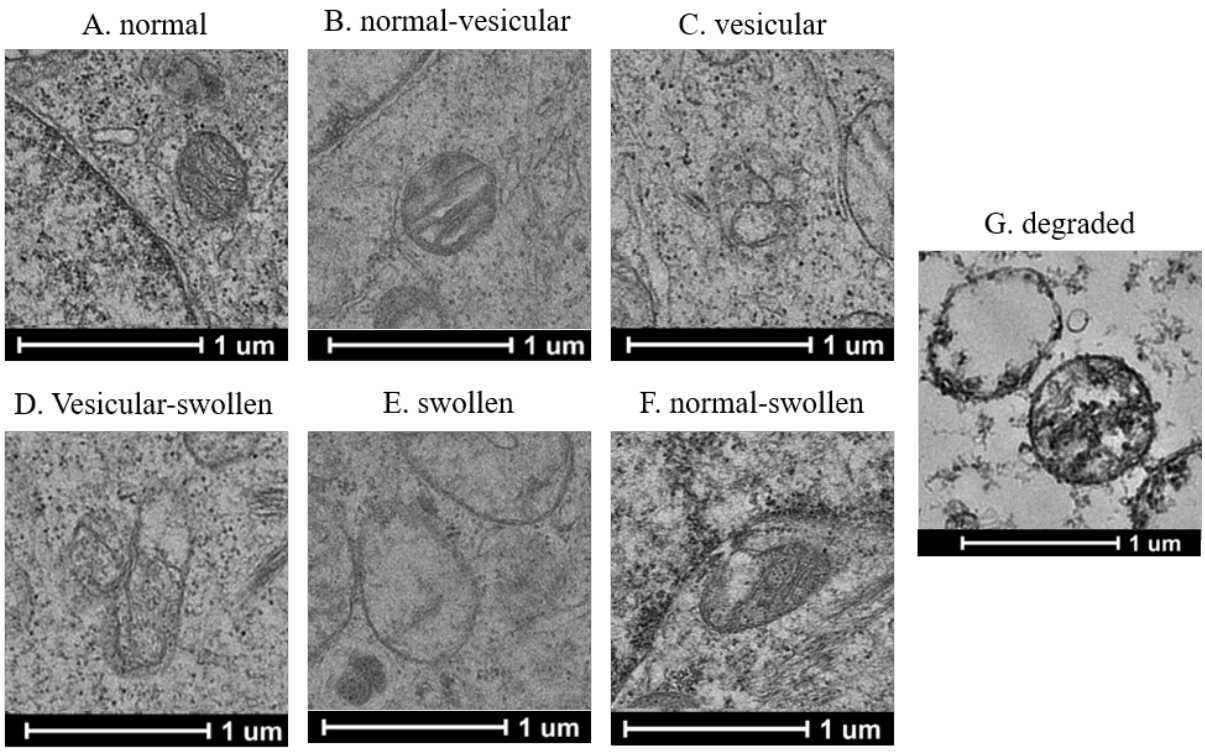

Figure 6. AgNPs effect mitochondrial ultrastructure. Representative TEM images of mitochondria in each cristae category. Examples of A) normal mitochondria with normal cristae, B) normal-vesicular cristae, C) vesicular cristae, D) vesicular-swollen cristae, E) swollen mitochondria with no discernable cristae, and F) normal-swollen cristae. G) 50 µg/ml Ag nitrate caused there to be no identifiable cellular structures and the mitochondria was categorized as degraded.

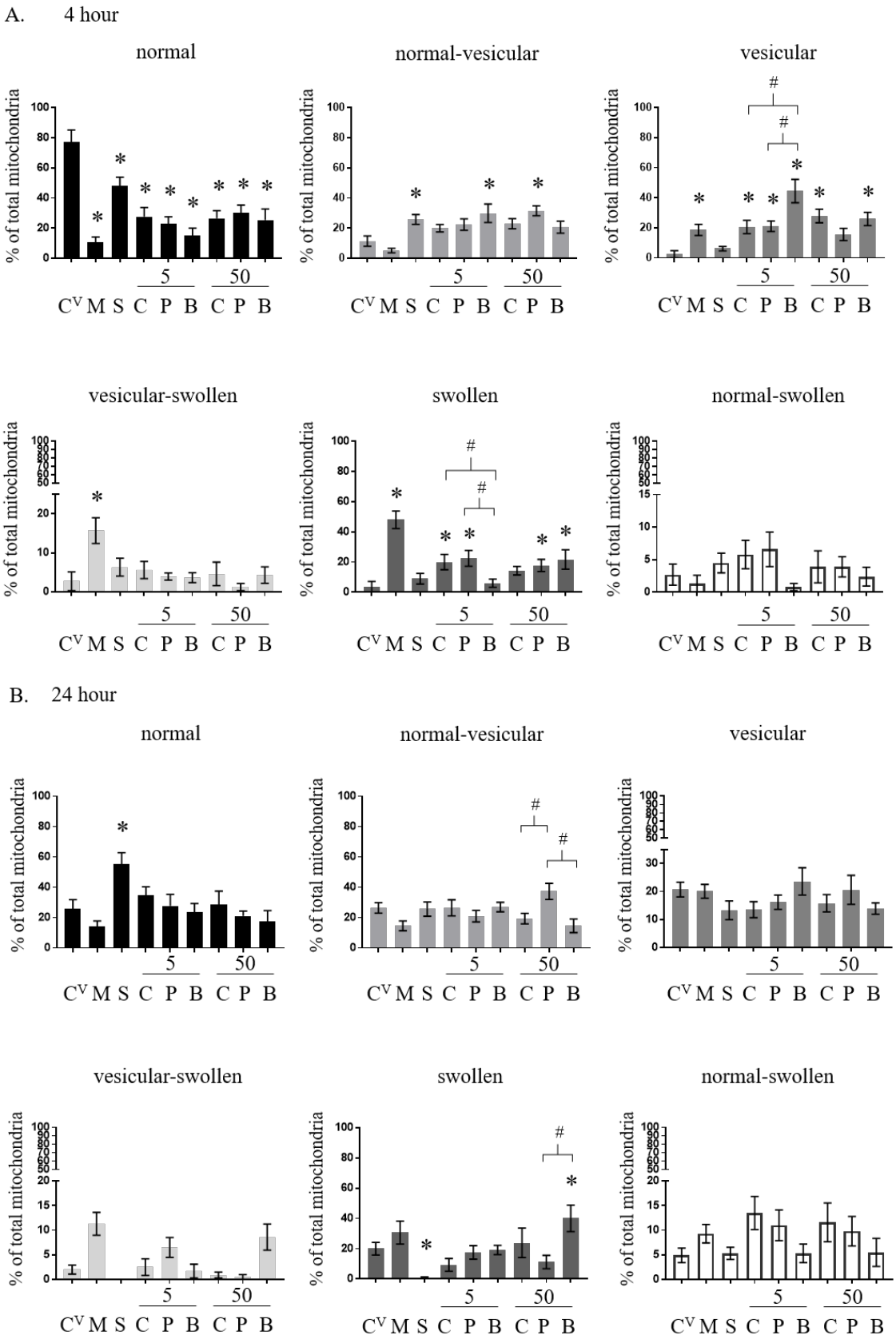

Figure 7. AgNPs effect mitochondrial ultrastructure. A) Percentage of total mitochondria within each cristae category after 4 hours and B) 24 hours. Data displayed is mean of total mitochondria from 10 cells analyzed per treatment with SEM. One way ANOVA with multiple comparison tests with * $p<0.05$ compared to control+vehicle using Dunnetts and # $p<0.05$ compared within concentration using Tukey. C^V=control+vehicle, M=80 µM mdivi-1, S=4 µM staurosporine, C=Ag citrate, P=Ag PVP, B=Ag BPEI

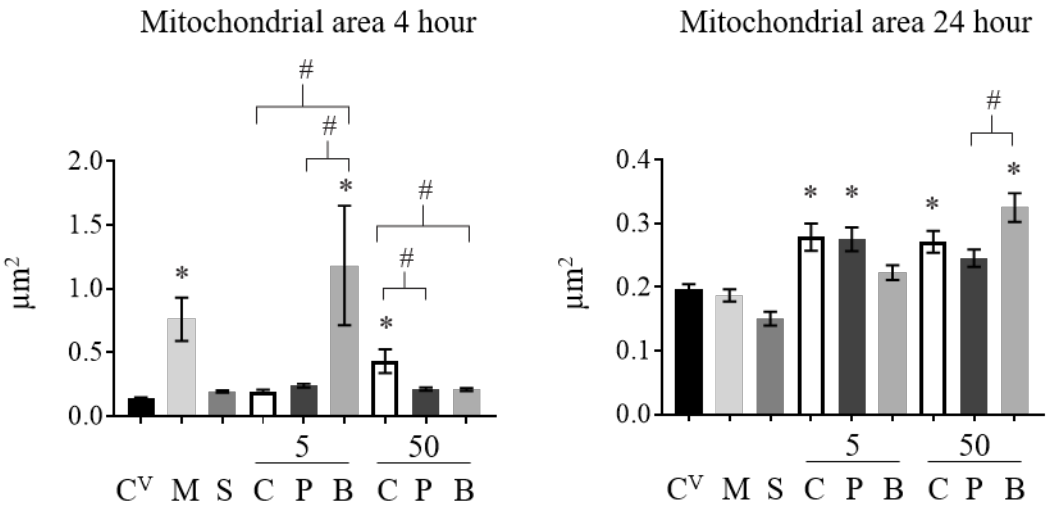

Figure 8. AgNPs effect mitochondrial area. Mitochondria with a roundness value ≥0.55 μm^2 were quantified as cross sections. Bar graphs display mean area of 150-200 mitochondria in cross section per treatment with SEM. One way ANOVA with multiple comparison tests with * $p<0.05$ compared to control+vehicle using Dunnetts and # $p<0.05$ compared within concentration using Tukey. C^V=control+vehicle, M=80 µM mdivi-1, S=4 µM staurosporine, C=Ag citrate, P=Ag PVP, B=Ag BPEI